 FDMP, vol.14, no.4, pp.281-291, 2018

# On the Control of the Master Cylinder Hydraulic Pressure for Electro-Hydraulic Brake (EHB) Systems with the Sliding Mode Design Methodology

**Qiping Chen[1,*], Yu Liu [1], Liping Zeng[1], Qiang Xiao[1], Conghui Zhou[1] and Sheng Kang[1]**

**Abstract:** The brake-by-wire system requirement is promoted owing to the development of green energy vehicle, and the brake pressure control method is needed. A control method for the master cylinder hydraulic pressure based on the sliding mode control approach is proposed to provide the Electro-Hydraulic Brake system (EHB) of electric vehicles with superior system performances. An assessment is carried out about the complex nonlinear characteristics and sensitivity to the external environment of these systems, which include illustrating the working principle of the EHB system, establishing the dynamic models of the key components of the EHB system. The sliding mode control method is designed after introducing relevant dynamic models for the related key components. In particular, three kinds of wheel cylinder hydraulic response curves under different braking conditions (Normal braking conditions, Emergency braking conditions, and Failure safety protection braking conditions) are considered. The simulation results show that the sliding mode control method for the master cylinder under the EHB system has strong pressure-building capability, short response time and superior system performance Therefore, the sliding mode control method proposed in this paper is an ideal method for master cylinder hydraulic pressure control under the EHB system and has a wide range of engineering application for electric vehicles.

**Keywords:** Electric vehicles, the EHB system, master cylinder, hydraulic pressure, sliding mode control.

## 1 Introduction

Electrification and intelligence of vehicle promotes the brake system, which needs to use brake-by-wire technology. Electro-hydraulic braking system used in electric vehicles embodies the advantages of safety, comfort, quick response, regenerative braking and precise braking force control [Yu, Han, Xu et al. (2017)]. However, due to the complex nonlinear characteristics of vehicle braking systems, it is difficult to accurately control the hydraulic pressure [Haba and Oancea (2015)]. Therefore, it is necessary to propose the EHB system hydraulic pressure control method that can establish a brake pressure of

[1] Key Laboratory of Conveyance and Equipment Ministry of Education, East China Jiaotong University, Nanchang, 330013, China.

[*] Corresponding Author: Qiping Chen. Email: qiping3846758@163.com.

100 bars in less than 170 ms.

A large number of studies about the EHB system have been carried out at home and abroad, Yu et al. [Xiong, Lin, Yu et al. (2016)] designed an integrated electro-hydraulic brake system, using Byrnes-Isidori standard method to analyze the system, whose system response is quick and has great control precision. Xiong et al. [Xiong, Lin, Yu et al. (2016)] proposed a dual-powered electro-hydraulic braking system. The simulation results demonstrate that the system's ability satisfies the design requirements and the system is superior to the existing electro-hydraulic braking system. However, the dual-powered the EHB system's response time is slow. Li et al. [Li, Ma, Guo et al. (2015)] established AMEsim model of the EHB system, but it also needs to improve road surface adhesion coefficient estimation based on the non-linear least squares. Oshima et al. [Oshima, Fujiki and Nakao (2011)] directly took the hydraulic pressure of the EHB system master cylinder as a variable control, which is easy to observe and does not require excessive modification to the brake system. However, it cannot achieve accurate control in the low-pressure range. Yong et al. [Yong, Gao, Ding et al. (2017)] designed a new type of electro-hydraulic brake system (E-booster) and verified the performance of the system by Hardware-in-the-loop simulation. It has superior braking capacity and good braking pedal feel, but lack of systematic study of its stability control and regenerative braking.

Based on the analysis of the EHB system and its nonlinear characteristic, a dynamic model of key components of the EHB system and an experimental model based on the co-simulation platform are established. According to the complex features of the EHB system hydraulic pressure control, a sliding mode control method with good robustness is proposed to achieve rapid brake pressure response and precise pressure control.

## 2 Operating principle of the EHB system

The EHB system configuration is shown in Fig. 1. The EHB system generally consists of a pedal simulator, a pressure building unit in the form of motor-driven deceleration mechanism, a hydraulic control unit, a failure safety protection system and a brake line [Xiong, Xu and Yu (2016)]. When all solenoid valves are normally operated, the system obtains the driver's braking intention through the pedal displacement sensor. According to the actual working condition, the ECU calculates the required hydraulic braking force, then the force can be converted to the amount of torque the motor needs. After that, the motor generates the corresponding torque through the deceleration mechanism and drives the master cylinder push rod building pressure. When the EHB system fails, the ECU shuts off all solenoids valve and the system turns to failure safety protection mode. The secondary master cylinder and the brake wheel cylinder are directly related. After the brake pedal is depressed, the brake fluid flows directly to the brake wheel cylinder from the secondary master cylinder and achieves braking.

1-ECU; 2-battery; 3-motor; 4-bevel gear drive unit; 5-gear; 6-rack; 7-push rod; 8-first piston of brake master cylinder; 9-first working chamber of brake master cylinder; 10-liquid storage tank; 11-secondary piston of brake master cylinder; 12-second working chamber of brake master cylinder; 13-brake master cylinder; 14-ABS/ESP; 15-switch valve; 16-pedal simulator; 17-control valve; 18-hydraulic pressure sensor 1; 19-hydraulic pressure sensor 2; 20-mode switching valve; 21-secondary master cylinder; 22-pedal push rod; 23-pedal displacement sensor; 24-pedal.

The EHB system, as showed in Fig. 1, adopts the form of two-stage decelerating mechanism that includes a bevel gear pair and gear and rack to achieve the purpose of deceleration and increasing torque. At the same time, the rotational movement of a motor is converted into the linear movement of a push rod in the master cylinder. The parameters of deceleration mechanism are shown in Tab. 1.

**Table 1:** Deceleration mechanism parameters

| Project | Value |
|---|---|
| The teeth of small bevel gear | 20 |
| The teeth of large bevel gear | 80 |
| The module of bevel gear (mm) | 3 |

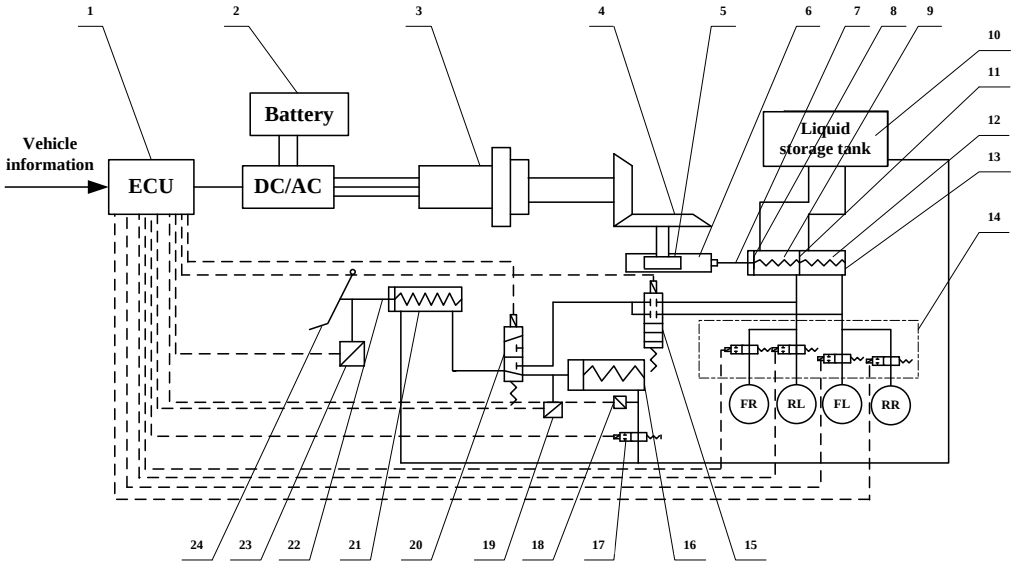


**Figure 1:** The EHB system configuration

## 3 Analysis of the EHB system

### *3.1 Modeling of the EHB system*

The dynamic mode of the motor and deceleration mechanism is established, which is shown in Eqs. (1), (2) and (3). The deceleration mechanism is in the form of a gear transmission and ball screw transmission.

$$J_m \ddot{\theta}_m + C_m \dot{\theta}_m = T_m - T_s \tag{1}$$

$$J_s \ddot{\theta}_s + C_s \dot{\theta}_s = iT_s - T_r \tag{2}$$

$$m_c \ddot{x}_r + b_r \dot{x}_r = T_r \frac{2\pi}{p_h} - p_{11} S_1 \tag{3}$$

Here, $J_m$ is rotary inertia of motor and small gear, $C_m$ is damping coefficient of motor shaft, $T_m$ is output torque of motor, $T_s$ is torque of small gear, $\theta_m$ is rotation angle of the motor shaft, $J_s$ is rotary inertia of large gear and screw nut, $C_s$ is rotational damping coefficient of large gear and screw nut, $\theta_s$ is rotation angle of large gear, $i$ is reduction ratio of first deceleration mechanism, $T_r$ is torque of nut end region, $m_c$ is mass of lead screw, $x_r$ is displacement of lead screw, $b_r$ is damping of lead screw, $p_h$ is the lead of ball screw, $p_{11}$ is pressure intensity of first working chamber of brake master cylinder, and $S_1$ is internal area of brake master cylinder.

According to three different work stages, respectively a dynamic model of the master cylinder is established, which is shown in Eqs. (4), (5), (6) and (7) [Wan (2015)].

$$(M_{m1}+M_{m2})\ddot{x}_1+C_{m2}\dot{x}_1+k_{m2}x_1=F_f-F_{m20}-F_{f1}-F_{f2}-P_2A \tag{4}$$

$$M_{m1}\ddot{x}_1+C_{m1}(\dot{x}_1-\dot{x}_2)+k_{m1}(x_1-x_2)=F_f-F_{f1}-P_1A \tag{5}$$

$$M_{m2}\ddot{x}_2+C_{m2}\dot{x}_2+k_{m2}x_2=C_{m1}(\dot{x}_1-\dot{x}_2)+k_{m1}(x_1-x_2)-F_{f2}-P_2A+P_1A \tag{6}$$

$$M_{m1}\ddot{x}_1+C_{m1}\dot{x}_1+k_{m1}x_1=F_f-F_{f1}-P_2A \tag{7}$$

Here, $M_{m1}$ is the first piston mass, $M_{m2}$ is the second piston mass, $x_1$ is the first piston displacement, $x_2$ is the second piston displacement, $C_{m1}$ is spring damp coefficient of front chamber, $C_{m2}$ is spring damp coefficient of rear chamber, $k_{m1}$ is spring stiffness of front chamber, $k_{m2}$ is spring stiffness of rear chamber, $F_f$ is the thrust first piston received, $F_{f1}$ is the friction force of the first piston received, $F_{f2}$ is the friction force of the second piston received, $F_{m20}$ is precipitating force of the rear chamber spring, $P_1$ is pressure of front chamber, $P_2$ is pressure of rear chamber, and $A$ is piston area.

The continuous flow equation of the first brake chamber is established, which is shown in Eq. (8):

$$\frac{dp_1}{dt}=\frac{k_e}{v_1}(s_{m1}\dot{x}_1-Q_1-r_m p_1) \tag{8}$$

Here, $k_e$ is brake fluid equivalent to volume elastic modulus in the master cylinder, $Q_1$ is valve port flow between the first brake chamber and brake line, $v_1$ is the initial volume of the first brake chamber, $s_{m1}$ is piston area of the first brake chamber, and $r_m$ is leakage coefficient of the first brake chamber.

The continuous flow equation of the second brake chamber is established, which is shown in Eq. (9).

$$\frac{dp_2}{dt} = \frac{k_e}{v_2}(s_{m2}\dot{x}_2 - Q_2 - r_{m2}p_2) \tag{9}$$

Here, $Q_2$ is valve port flow between the second brake chamber and brake line, $v_2$ is the initial volume of the second brake chamber, $s_{m2}$ is piston area of the second brake chamber, and $r_{m2}$ is leakage coefficient of the second brake chamber.

Dynamic model of brake fluid is established, which is shown in Eqs. (10), (11) and (12) [Feng, Gong and Yang (2010)].

$$k_e = \frac{1}{A\alpha^2 + B\alpha + 1}k_1 \tag{10}$$

$$A = -10\delta_0 k_1 (\frac{p_0}{p})^{\frac{1}{r}} \tag{11}$$

$$B = 10\delta_0 k_1 (\frac{p_0}{p})^{\frac{1}{r}} + \frac{1}{p - p_0}[1 - (\frac{p_0}{p})^{\frac{1}{r}}]k_1 - 1 \tag{12}$$

Here, $k_1$ is bulk modulus of pure brake fluid, $\delta_0$ is air solubility under the standard atmospheric pressure, $r$ is gas adiabatic coefficient, $\alpha$ is actually gas content in brake fluid, and $p_0$ is the standard atmospheric pressure.

Based on the co-simulation experiment platform of AMEsim and Simulink, the co-simulation model is established, as shown in Fig. 2. Because of lacking ball screw module in AMEsim, rack pinion is the replacement. The control module built by Simulink accepts the displacement of the pedal and the pressure of the pipe, and the output is the torque signal of the two motors.

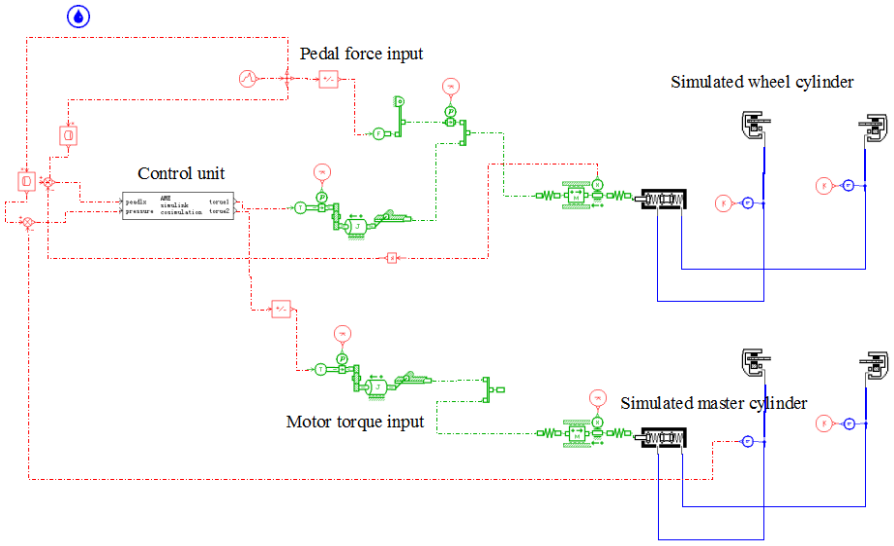


**Figure 2:** Co-simulation model

### *3.2 Control method of the EHB system*

The EHB system control method uses the driver's pedal force as the control input sign, with the brake master cylinder push rod displacement $x_1$ and pipeline hydraulic pressure $p$ as the feedback to control the output torque of the motor. The control logic diagram is shown in Fig. 3. Because of the nonlinear problem of braking system [Yuan, Fan, Yuan et al. (2017)], the sliding mode control with good robustness is adopted [Young, Utkin and Ozguner (1999)].

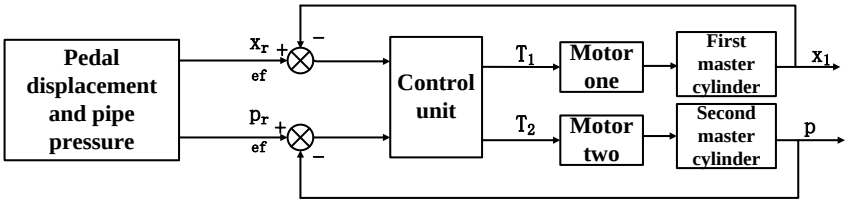


**Figure 3:** Control logic diagram

In the variable structure control system, the system has two stages of motion, one is the approaching process that reaches the switch surface from the initial state, and the other is the maintaining process that stays in the sliding mode [Li, Shi, Yao et al. (2016)]. Sliding mode control is a kind of control strategy of the variable structure control system which is characterized by discontinuous control [Edwards and Shtessel (2016)]. The control strategy can force the system to achieve a man-designed sliding mode, which is independent of system parameters and external disturbances.

The general nonlinear systems are shown in Eq. (13) [Li, Wang and Shi (2016)].

$$\dot{x} = f(x,u,t) \tag{13}$$

Here, $x$ is the state variable, and $u$ is the control variable.

Let's take the brake master cylinder as an example. Because the pressure difference between the front and rear chambers of the master cylinder is not big, and the damping force and spring force compared to the pod thrust is small. It can be considered as an external disturbance, so the master cylinder dynamic equation can be simplified as below:

$$M_{m1}\ddot{x}_1 = F_f - p_1 A \tag{14}$$

Pressure $p_1$ and displacement $x_1$ have the following polynomial fitting relationship, which is shown in Eq. (15).

$$p_1 = \left(\frac{x_1 - 0.97}{74.1}\right)^4 \tag{15}$$

Taking motor torque $u(t)$ as a control variable, the system equation is shown in Eq. (16).

$$\ddot{x}_1 = \frac{r}{M_{m1}}u(t) - \frac{\left(\frac{x_1 - 0.97}{74.1}\right)^4 A}{M_{m1}} \tag{16}$$

Here, $r$ is reduction ratio of the decelerating mechanism.

Defining the system's state variables, which is shown in Eq. (17).

$$e = x_{ref} - x_1 \tag{17}$$

Here, $x_{ref}$ is the master cylinder rod reference displacement.

The sliding surface function is defined, as shown in Eq. (18).

$$s = e \tag{18}$$

Based on the exponential approaching law, the approaching function is obtained, as shown in Eq. (19).

$$\dot{s} = -\varepsilon \operatorname{sgn}(s) - qs \tag{19}$$

Here, $\varepsilon$ and $q$ are parameters of the sliding mode controller. If $\varepsilon$ is small enough, the system jitter can be reduced.

Finally, the master cylinder push rod displacement $x_1$ can be obtained as the state variables. The motor torque $u(t)$ can be obtained as the control variable. The controller equation is shown in Eq. (20).

$$u = \frac{M_{m1}}{r}\frac{\partial(-\varepsilon \operatorname{sgn}(s) - qs)}{\partial t} + \frac{A}{r}\left(\frac{x_1 - 0.97}{74.1}\right)^4 \tag{20}$$

The brake pipe hydraulic pressure $p$ can be obtained as the state variable. The motor torque $u(t)$ can be obtained as the control variable. The controller equation is established, as shown in Eq. (21).

$$u = \frac{M_{m1}}{r}\frac{\partial(-\varepsilon \operatorname{sgn}(s) - qs)}{\partial t} + \frac{A}{r}p \tag{21}$$

The Simulink simulation block diagram of sliding mode controller is established, as shown in Fig. 4.

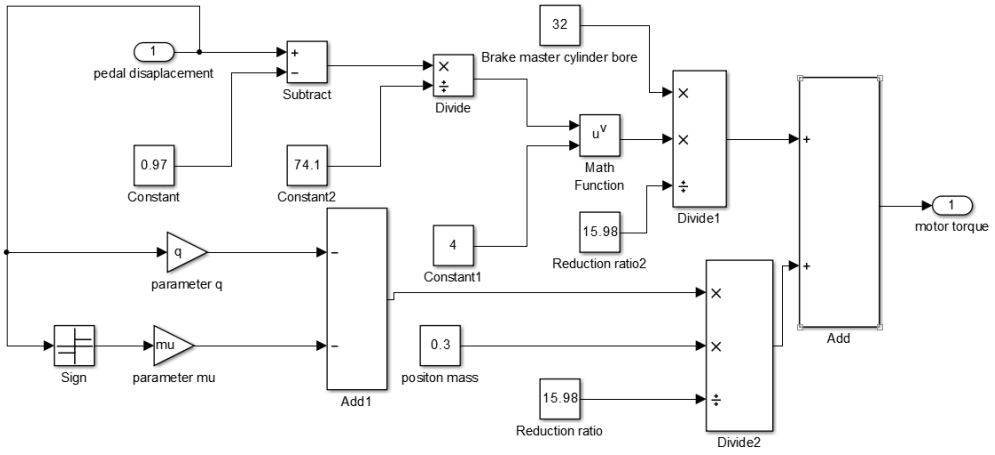


**Figure 4:** Simulink simulation block diagram of sliding mode controller

## 4 Simulation analysis

### *4.1 Normal braking conditions*

During vehicle braking, most of the working conditions possess small or medium-sized strength. In general, 0~0.5 g brake intensity conditions account for 95% of vehicle braking conditions. Therefore, the brake condition which is higher than the 0.8 g brake intensity can be regarded as the emergency braking conditions, and the break lower than 0.8 g brake intensity can be regarded as the normal braking conditions.

When the EHB system simulation under the normal braking conditions is running, the step input is 50 N pedal force, and the step time is delayed by 0.1 s to simulate the driver reaction time during actual driving. The expected hydraulic pressure response is 100 bars. According to the brake pedal force and pedal displacement relationship meeting the requirements of pedal feel, the corresponding pedal displacement is 42.27 mm. The simulation time is set as 1.5 s, and hydraulic responses under normal braking conditions is shown in Fig. 5. Fig. 5 shows that the control method could get a rapid, steady and less vibration response under the 50 N pedal forces as step input. After the driver presses the pedal, within 0.2 s, the pressure of the wheel cylinder can reach a stable 94.30 bars, and the root mean square error (RMSE) is 13.4608 bars.

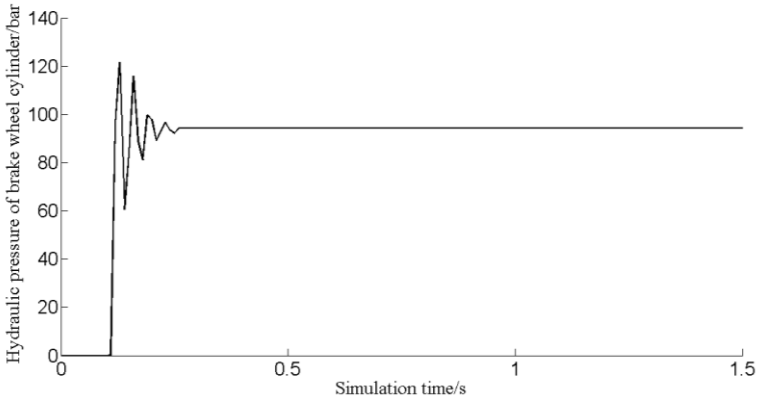


**Figure 5:** Hydraulic responses under normal braking conditions

### *4.2 Emergency braking conditions*

When a vehicle encounters emergency condition, the driver may press the pedal rapidly. The system will shift into emergency braking conditions, when ECU judging brake intensity is over 0.8 g. When the simulation test under the emergency braking conditions is running, to get close to the real braking effect, pedal input is zero value. Hydraulic braking force is entirely provided by the motor-driven deceleration mechanism. The motor receives the step signal 1.6 N.m, and the expected hydraulic pressure response is 100 bars. The simulation result is shown in Fig. 6.

Fig. 6 shows that the motor obtains a step signal of 1.6 N·m, the system braking pressure can reach 110 bars within 0.3 s, and the RMSE is 18.7651 bars. Although in the initial stage, the brake pressure lags due to the motor response, resulting in a period of decrease. But after that the pressure builds rapidly, and the built pressure effect is also relatively

good. In a word, the system braking pressure can meet the requirements of emergency braking conditions.

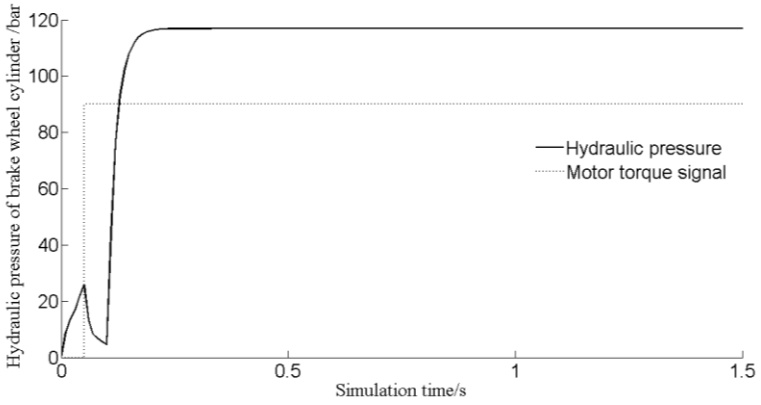


**Figure 6:** Hydraulic responses under emergency braking conditions

### *4.3 Failure safety protection braking conditions*

ECE R13 regulations state that the minimum remaining braking performance of braking system should generate a 2.9 m/s$^2$ braking deceleration within 500N brake pedal force. That is to say, the brake system generates a brake pressure, which is not less than 38 bars within 500 N brake pedal force. When the simulation under the failure safety protection braking condition is running, the step input is 500 N, which is regarded as the pedal force. The motor does not offer braking torque. The expected hydraulic pressure response is 60 bars, the hydraulic response under failure safety protection braking condition is shown in Fig. 7. Fig. 7 shows that after the braking operation, 60 bars can be obtained within 0.1 s, which is the maximum hydraulic pressure. After 0.2 s, the hydraulic pressure reaches to a stable value at 54.3 bars. And the RMSE is 13.6734 bars. Pressure building capability exceeds 38 bars needed by regulatory requirements. It can be concluded that the EHB system has failure safety protection redundancy, which can satisfy the braking requirements.

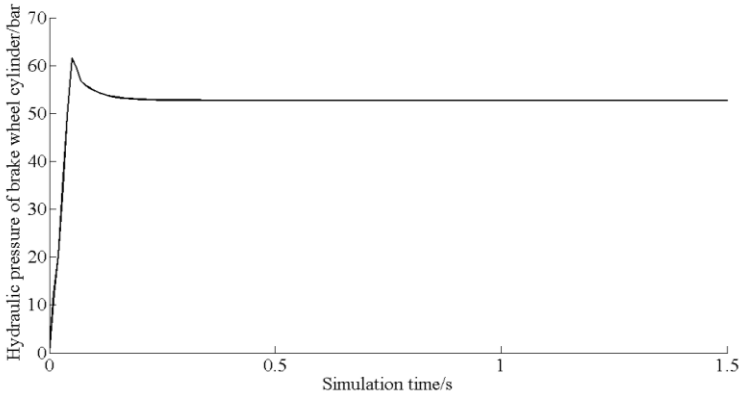


**Figure 7:** Hydraulic response under failure safety protection braking conditions

## 5 Conclusions

(1) In order to make the EHB system meet design criteria supporting a brake pressure of 100 bars within 170 ms, the structure and working principle of the EHB system have been analyzed, a mathematical model of the key components of the EHB system has been elaborated, and a sliding mode control algorithm has been proposed as feedback control for the motor output torque.

(2) In order to verify the feasibility of the sliding mode control algorithm, a simulation model has been introduced, based on the co-simulation experiment platform of AMEsim and Simulink. Normal braking conditions, emergency braking conditions and failure safety protection braking conditions have been simulated and analyzed. According to the simulation results, the EHB system has good pressure-building capability and short response time, which indicates that the sliding mode control method proposed in this paper could be an ideal method for the control of the master cylinder hydraulic pressure in EHB systems.

**Acknowledgements:** The authors would like to thank anonymous reviewers for their helpful comments and suggestions to improve the manuscript. This research was supported by the National Natural Science Foundation of China (Grant No. 51565011), and the Natural Science Foundation for Distinguished Young Scholars of Jiangxi province (Grant No. 20171BCB23059), and the Key Research Program of Jiangxi Province (Grant No. 20171BBE50039), and the Natural Science Foundation of Jiangxi Province (Grant Nos. 20171BAB216027 and 20171BAB216029), and the Foundation of Communications Department of Jiangxi Province (Grant No. 2015D0065).

## References

**Edwards, C.; Shtessel, Y. B.** (2016): Adaptive continuous higher order sliding mode control. *Automatica*, vol. 65, no. 3, pp. 183-190.

**Feng, B.; Gong, G.; Yang, H.** (2010): Method and experiment of elastic modulus increase of hydraulic oil. *Journal of Agricultural Machinery*, vol. 41, no. 5, pp. 219-222.

**Haba, S. A.; Oancea, G.** (2015): Digital manufacturing of air-cooled single-cylinder engine block. *International Journal of Advanced Manufacturing Technology*, vol. 80, no. 8, pp. 747-759.

**Li, H.; Shi, P.; Yao, D.; Wu, L.** (2016): Observer-based adaptive sliding mode control for nonlinear Markovian jump systems. *Automatica*, vol. 64, no. 3, pp. 133-142.

**Li, H.; Wang, J.; Shi, P.** (2016): Output-feedback based sliding mode control for fuzzy systems with actuator saturation. *IEEE Transactions on Fuzzy Systems*, vol. 24, no. 6, pp. 1282-1293.

**Li, S.; Ma, Y.; Guo, P.; Zong, F.; Zhang, H.** (2015): Control strategy of vehicle stability based on electronically controlled hydraulic braking system. *Journal of Jilin University (Engineering and Technology Edition)*, vol. 45, no. 2, pp. 526-532.

**Oshima, T.; Fujiki, N.; Nakao, S.** (2011): Development of an electrically driven intelligent brake system. *SAE International Journal of Passenger Cars-Mechanical Systems*, vol. 4, no. 1, pp. 399-405.

**Wan, Y.** (2015): *Electronic Hydraulic Braking System Modeling and Hydraulic Pressure Dynamic Control (Ph. D. Thesis)*. Tongji University.

**Xiong, L.; Lin, J.; Yu, Z.; Xu, S.** (2016): Research on electro-hydraulic braking system with dual power sources. *Automotive Engineering*, vol. 38, no. 6, pp. 745-753.

**Xiong, L.; Xu, S.; Yu, Z.** (2016): Optimal hydraulic pressure control of electronic hydraulic braking system based on flutter compensation. *Journal of Mechanical Engineering*, vol. 52, no. 12, pp. 100-106.

**Young, K. D.; Utkin, V. I.; Ozguner, U.** (1999): A control engineer's guide to sliding mode control. *IEEE Transactions on Control Systems Technology*, vol. 7, no. 3, pp. 328-342.

**Yong, J.; Gao, F.; Ding, N.; He, Y.** (2017): Design and validation of an electro-hydraulic brake system using hardware-in-the-loop real-time simulation. *International Journal of Automotive Technology*, vol. 18, no. 4, pp. 603-612.

**Yu, Z.; Han, W.; Xu, S.; Xiong, L.** (2017): Review on hydraulic pressure control of electro hydraulic brake system. *Journal of Mechanical Engineering*, vol. 49, no. 6, pp. 90-102.

**Yu, Z.; Han, W.; Xiong, L.; Xu, S.** (2016): Hydraulic force control of integrated electro hydraulic brake system based on Byrnes-Isidori standard. *Journal of Mechanical Engineering*, vol. 52, no. 22, pp. 92-100.

**Yuan, C.; Fan, X.; Yuan, H.; Shen, J.; Chen, L. et al.** (2017): Design and test of parallel electrically controlled hydraulic braking system for smart vehicles. *Journal of Agricultural Machinery*, vol. 48, no. 5, pp. 369-376.